Gaussian Mixture Modeling of Acoustic Emissions for Structural Health Monitoring of Reinforced Concrete Structures

Alireza Farhidzadeh, Ehsan Dehghan-Niri, Salvatore Salamone*

Smart Structures Research Laboratory (SSRL), Department of Civil, Structural, and Environmental Engineering, University at Buffalo, The State University of New York, 212 Ketter Hall, Buffalo, NY, USA 14260

ABSTRACT

Reinforced Concrete (RC) has been widely used in construction of infrastructures for many decades. The cracking behavior in concrete is crucial due to the harmful effects on structural performance such as serviceability and durability requirements. In general, in loading such structures until failure, tensile cracks develop at the initial stages of loading, while shear cracks dominate later. Therefore, monitoring the cracking modes is of paramount importance as it can lead to the prediction of the structural performance. In the past two decades, significant efforts have been made toward the development of automated structural health monitoring (SHM) systems. Among them, a technique that shows promises for monitoring RC structures is the acoustic emission (AE). This paper introduces a novel probabilistic approach based on Gaussian Mixture Modeling (GMM) to classify AE signals related to each crack mode. The system provides an early warning by recognizing nucleation of numerous critical shear cracks. The algorithm is validated through an experimental study on a full-scale reinforced concrete shear wall subjected to a reversed cyclic loading. A modified conventional classification scheme and a new criterion for crack classification are also proposed.

Key words: Acoustic Emission, Crack mode classification, Cluster Analysis, Gaussian Mixture Modeling, Probabilistic damage diagnosis, Reinforced concrete.

1. INTRODUCTION

Structures made of reinforced concrete (RC) are ubiquitous in modern infrastructure systems. These structures are subjected to deterioration due to aging, increased load, and natural hazards. Conventionally, the assessment of civil structures relies on visual inspection (VI) [1], which in some cases is accompanied with some form of ground-based nondestructive evaluation (NDE) method. Nonetheless, severe degradation could go undetected. Notable examples of such unanticipated failures that have exposed shortcomings in current assessment methodologies can be found worldwide, such as the viaduct of the Belfast-Dublin railway line collapsed in 2009 and the Christchurch CBD buildings collapsed in 2011 [2,3]. Structural health monitoring is a field that has received significant interest over the past few years and has led to the development of a wide variety of systems that can overcome the qualitative nature of VI-based condition assessment [4–13]. In particular a technique that shows promises for monitoring crack propagation in RC structures is Acoustic Emission (AE). The past few years have seen a surge of research aim at determining functional or correlation interdependencies between crack characteristics and AE features [4,14], including *b*-value and Sifted *b*-value (S*b*) analysis [5,8,15] and AE energy [16]. In this paper a new approach based on a Gaussian Mixture Modeling (GMM) is presented. GMM is an *unsupervised distribution-based classification* technique [17] that has been successfully used in many fields, including sound recognition [18,19], image processing [20], dynamical systems and tracking [21], and text recognition [22]; however the application of this method in AE-based structural health monitoring (SHM) systems has not been investigated. Such system, coupled with remote facilities [23], could be employed to continuously monitor complex structures and alleviate hundreds of inspection obstacles stemming from accessibility restrictions, complex geometries, and the location of hidden damage. The rest of this paper is organized as follow: the next section describes the

* ssalamon@buffalo.edu; phone: +1(716) 645-1523, fax: +1(716) 645-3667

Sensors and Smart Structures Technologies for Civil, Mechanical, and Aerospace Systems 2013, edited by Jerome Peter Lynch, Chung-Bang Yun, Kon-Well Wang, Proc. of SPIE Vol. 8692, 86920B · © 2013 SPIE · CCC code: 0277-786X/13/$18 · doi: 10.1117/12.2008705

conventional crack classification in RC structures and its drawbacks. The novel approach and the theory behind GMM are then given in section 3. Experimental setup is explained in section 4 followed by the results of structural response and AE monitoring in section 5. Finally conclusions are summarized in section 6.

2. CONVENTIONAL CLASSIFICATION

Extracting features from AE signals is usually referred to as parameter-based technique. The Japan Construction and Material Standard (JCMS) [24] proposed a technique to monitor the crack propagation in concrete structures based on two AE parameters, namely "Average Frequency (AF)" and "RA" value. AF is defined as the ratio of *counts* to *duration* and RA is the proportion of *rise time* to *peak amplitude*. Figure 1 illustrates this conventional crack classification approach using these two features. In particular, a straight line recommended line to separate tensile signals from shear signals [5,7,25–28]. The JCMS technique is based on the observation that, in general tensile cracks generate AE waveforms with short rise-time and high frequency, whereas shear cracks usually result in longer rise-time with lower frequency and longer rise time [29]. Several experimental studies demonstrated the effectiveness of these two features [8,25,27–29]; however, it should be mentioned that a defined criterion on the proportion of RA value and average frequency (characteristics of the separator line in Figure 1) has not been established yet [5,7,27]. In this paper, a new probabilistic approach based on a Gaussian Mixture Modeling (GMM) is proposed to classify AE signals.

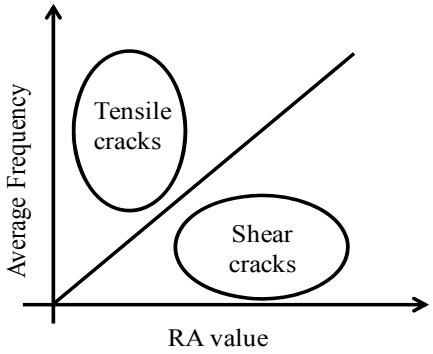

Figure 1. Conventional crack classification in JCMS-IIIB5706 code [24]

3. GAUSSIAN MIXTURE MODELING

A Gaussian Mixture Model is a parametric probability density function composed of weighted sum of *M* component Gaussian densities. For a *D*-dimensional observation or training vector $\vec{x}$, the mixture density is defined as [18],

$$p(\vec{x} \mid \lambda) = \sum_{i=1}^{M} \omega_i \, \mathcal{N}_i (\vec{x} \mid \vec{\mu}_i, \Sigma_i) \tag{1}$$

where ω_i, *i=1, ..., M,* are the mixture weights and $\mathcal{N}_i (\vec{x} \mid \vec{\mu}_i, \Sigma_i)$, *i = 1, ..., M*, are the component Gaussian (Normal) densities. Each component density is a *D*-variate Gaussian function of the form,

$$\mathcal{N}_i (\vec{x} \mid \vec{\mu}_i, \Sigma_i) = \frac{1}{(2\pi)^{D/2} \left| \Sigma_i \right|^{1/2}} \exp\left\{ -\frac{1}{2} (\vec{x} - \vec{\mu}_i)^T (\Sigma_i)^{-1} (\vec{x} - \vec{\mu}_i) \right\} \tag{2}$$

with D×1 mean vector $\vec{\mu}_i$, and D×D covariance matrix Σ_i. The mixture weights satisfy the constraint $\sum_{i=1}^{M} \omega_i = 1$. The parameters of a complete Gaussian mixture model are the mean vectors, covariance matrices and mixture weights from all component densities, represented together as,

$$\lambda = \{\omega_i, \vec{\mu}_i, \Sigma_i\}, \qquad i = 1, ..., M \tag{3}$$

The next step is to find the best estimate for λ using Maximum Likelihood (ML) [18, 30]. For a sequence of T training vectors $X = \{\vec{x}_1, ..., \vec{x}_T\}$, the GMM likelihood can be written as,

$$p(X \mid \lambda) = \prod_{t=1}^{T} p(x_t \mid \lambda) \tag{4}$$

ML parameters can be obtained iteratively by Expectation Maximization (EM) algorithm [30, 31]. This algorithm consists of two steps, Expectation and Maximization, which guarantees a monotonic increase in the model's likelihood value [31]. Expectation step produce the *a posteriori* probability for component *i*, which is defined as the probability of state *i* given the observation $\vec{x}_t$ and the k^{th} re-estimated model λ^k:

$$\Pr(i \mid \vec{x}_t, \lambda^k) = \omega_i \mathcal{N}(\vec{x}_t \mid \vec{\mu}_i^k, \Sigma_i^k) \Big/ \sum_{j=1}^{M} \omega_j \mathcal{N}(\vec{x}_t \mid \vec{\mu}_j^k, \Sigma_j^k) \tag{5}$$

The maximization step returns the distribution parameter with these components [18]:

$$\omega_i^{k+1} = \frac{1}{T} \sum_{t=1}^{T} \Pr(i \mid \vec{x}_t, \lambda^k) \tag{6}$$

$$\vec{\mu}_i^{k+1} = \left(\sum_{t=1}^{T} \Pr(i \mid \vec{x}_t, \lambda^k) \vec{x}_t \right) \Big/ \sum_{t=1}^{T} \Pr(i \mid \vec{x}_t, \lambda^k) \tag{7}$$

$$\Sigma_i^{k+1} = \left(\sum_{t=1}^{T} \Pr(i \mid \vec{x}_t, \lambda^k) \times (\vec{x}_t - \vec{\mu}_i^{k+1})(\vec{x}_t - \vec{\mu}_i^{k+1})^T \right) \Big/ \sum_{t=1}^{T} \Pr(i \mid \vec{x}_t, \lambda^k) \tag{8}$$

The use of a GMM is motivated by its capability to model some underlying set of hidden classes [18, 32, 33]. To implement a system for crack mode classification in concrete structures, the features (or measurement) is a 2-D vector (i.e., $\vec{x} = (RA, AF)$) and sequence of T training vectors is,

$$X = \{\vec{x}_1 = (RA_1, AF_1), ..., \vec{x}_t = (RA_t, AF_t), ..., \vec{x}_T = (RA_T, AF_T)\} \tag{9}$$

and the latent or hidden classes are i={1,2}, that is, tensile and shear mode, respectively.

4. EXPERIMENTAL SETUP

The specimen was a large scale RC shear wall with a height to width ratio of 0.94, designed based on ACI 318-08 [34]. Details about the specimen and AE setup are summarized in Table 1.

Table 1. Experimental details

RC shear wall		Acoustic emission	
Height [mm]	3300	AE system	PAC Micro-II
Width [mm]	3050	AE sensor	PAC R15α
Thickness [mm]	200	Number of sensors	8
Reinforcement Ratio [%]	0. 67	Preamplification [dB]	40
Concrete compressive strength f'_c [MPa]	24.8	Signal bandpass filter [kHz]	20-400
Reinforcing bars yield strength [MPa]	464	Trigger threshold [dB]	35
Reinforcing bars ultimate strength [MPa]	708	Sampling rate [MHz]	1

The main components of the AE system included an eight-channel high-speed data acquisition board (Physical Acoustics Corporation Micro-II PAC) and dedicated software for signal processing and storage (AEwin). AE sensors were attached to one face of the wall using hot glue. The experimental setup and sensor layout for loading test are shown in Figure 2.

Lateral load was applied to the specimen by two horizontally inclined high force capacity actuators. The specimen was subjected to a displacement controlled quasi-static reversed cyclic loading, see Table 2. Since very low AE activity was recorded prior to LS2, data in LS0 and LS1 was neglected in the post-processing analyses.

Table 2. Load protocol

Load step	**LS0**	**LS1**	**LS2**	**LS3**	**LS4**	**LS5**	**LS6**	**LS7**	**LS8**	**LS9**	**LS10**
Number of Cycles	3	2	2	2	2	2	2	2	2	2	2
Loading Time [sec]	2.5	3	6	9	12	16	20	30	40	60	80
Proposed displacement [mm]	1	1.9	3.8	5.7	7.6	10.2	12.7	19.1	25.4	38.1	50.8
Actual displacement [mm]	0.8	1.6	3.2	5.1	6.8	9.2	11.6	17.9	24.4	37.1	47.5

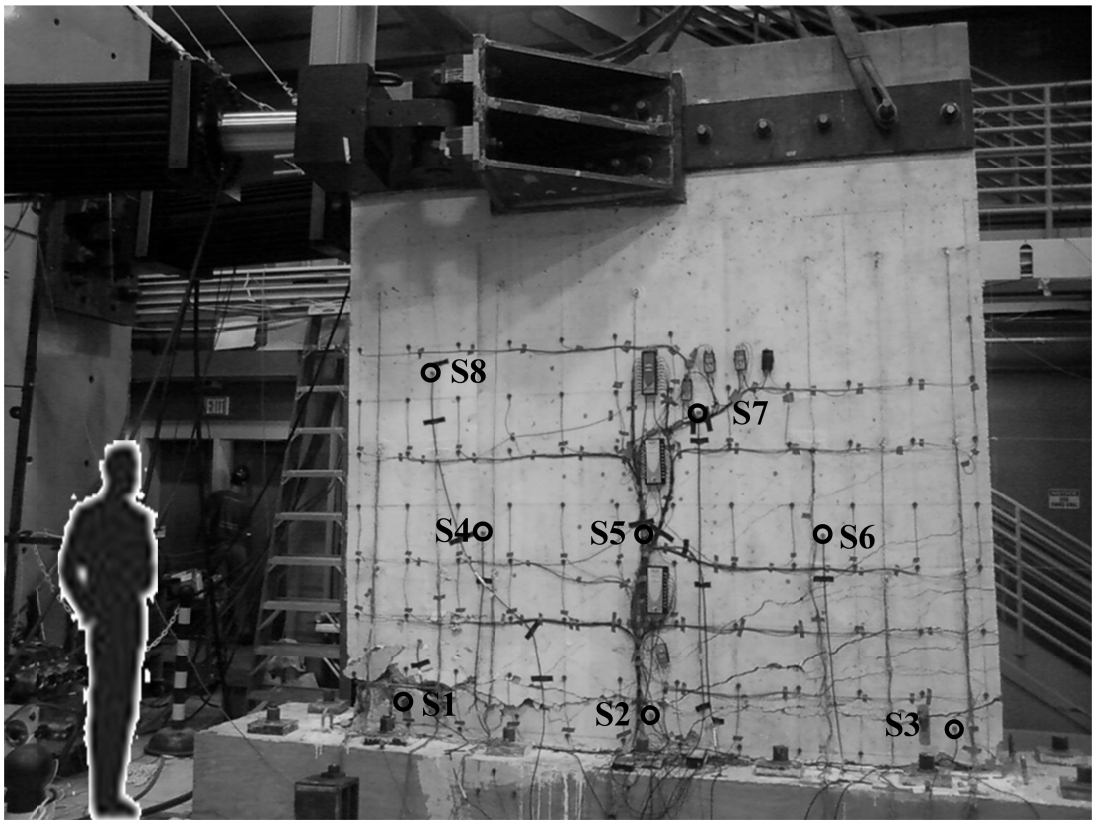

Figure 2. Laboratory test setup and AE sensor layout

5. RESULTS

5.1 Structural response

The force-displacement hysteresis loops and the corresponding backbone curves are illustrated in Figure 3. The specimen had a nonlinear response in LS7 and reached its ultimate strength in LS9. In the initial load steps the cracks started from tensile mode and then they were followed by diagonal shear cracks in the intermediate load steps. The diagonal cracks became dominant at the final load steps. A comprehensive report on the crack propagation pattern of this wall is available in [5] for interested readers.

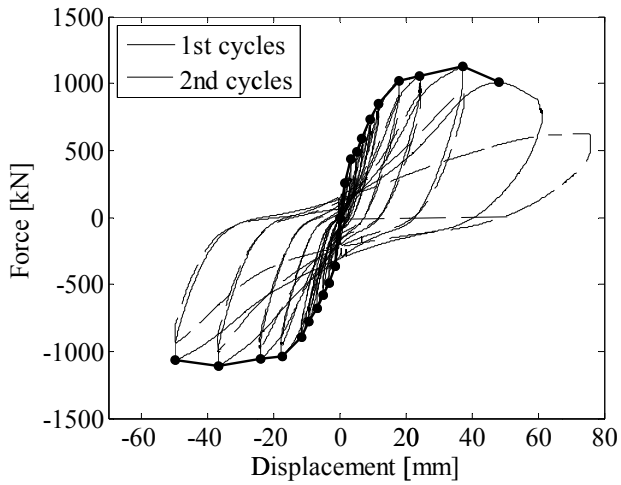

Figure 3. Force-displacement hysteresis loops and backbone curves [5]

5.2 GMM clustering outcome

This section presents the results of the crack classification approach using GMM. The observation dataset **X**, consisting of $x_i = (RA_i, AF_i)$ is $X = \{(RA_1, AF_1), (RA_2, AF_2), ..., (RA_n, AF_n)\}, x_i \in \mathbb{R}^2$. As an example, **X** for LS4 is shown in Figure 4. It can be observed that, using the JCMS classification scheme, establishing the best line to cluster the AE signals in two classes is not an easy task.

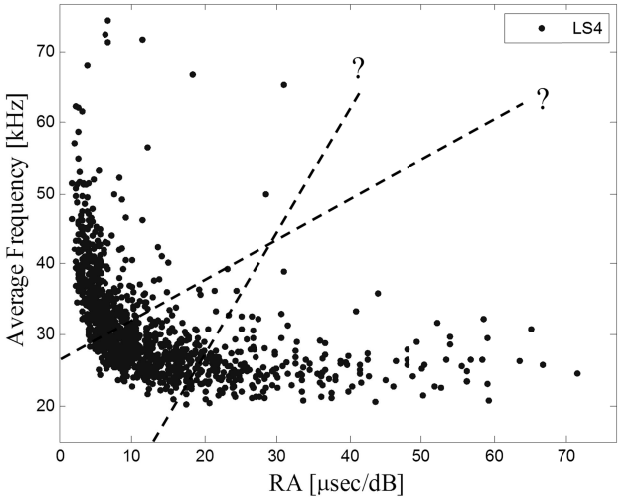

Figure 4. Typical pattern of Average Frequency vs. RA value and ambiguity of best separator line based on JCMS code

To overcome this limitation, the proposed clustering analysis was applied to partition the data set **X** in two subsets (i.e., i =1, 2), named cluster 1 (i.e., tensile cracks) and cluster 2 (i.e., shear cracks). The corresponding contour of Gaussian mixture density function at LS4 is illustrated in Figure 5. The following observation can be made: 1) the two hidden classes have a mixed Gaussian density function with a larger weight for the tensile class. This is the optimum equivalent of data set distribution with Gaussian mixture density, guaranteed by the GMM algorithm; 2) although we will propose a new criterion for clustering the two hidden classes, a line could be still used by defining the segment bisector of a virtual line that connects the means of each class. The example of this bisector is superimposed on Figure 5 by a dashed line. GMM analysis was carried out for each load step separately. Figure 6 illustrates the Gaussian mixture density functions at load steps 2, 5, 7, and 9. At LS2 as an initial load step, tensile cracks are clearly dominant. By increasing the applied load at intermediate load steps, e.g., LS5, shear signals start to increase as more diagonal cracks appear [5]. At LS7 almost all observations are clustered in shear mode as it is shown in Figure 6c with almost no secondary summit for Gaussian Mixture. At the final load steps (e.g., LS9), shear cluster begin to become fatter as shown by more topographical lines on

Figure 6d. These results confirmed three stages of crack mode propagation: dominancy of tensile cracks at the initial load steps, transition stage from tensile to shear in intermediate load steps, and dominancy of shear cracks at final load steps.

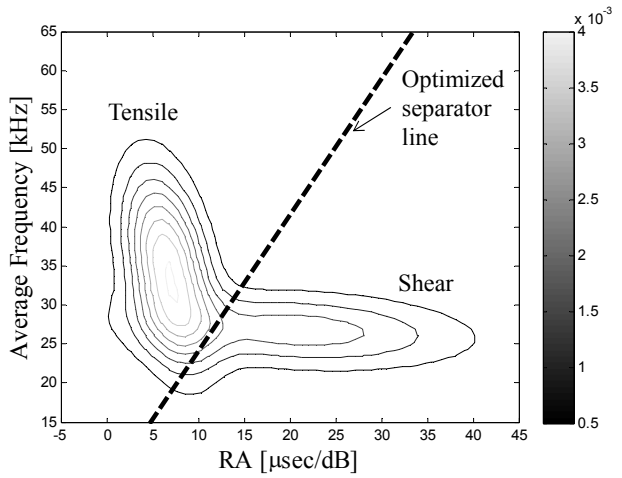

Figure 5. Mixed Gaussian density function of tensile and shear cracks at LS4 and the conventional separator line

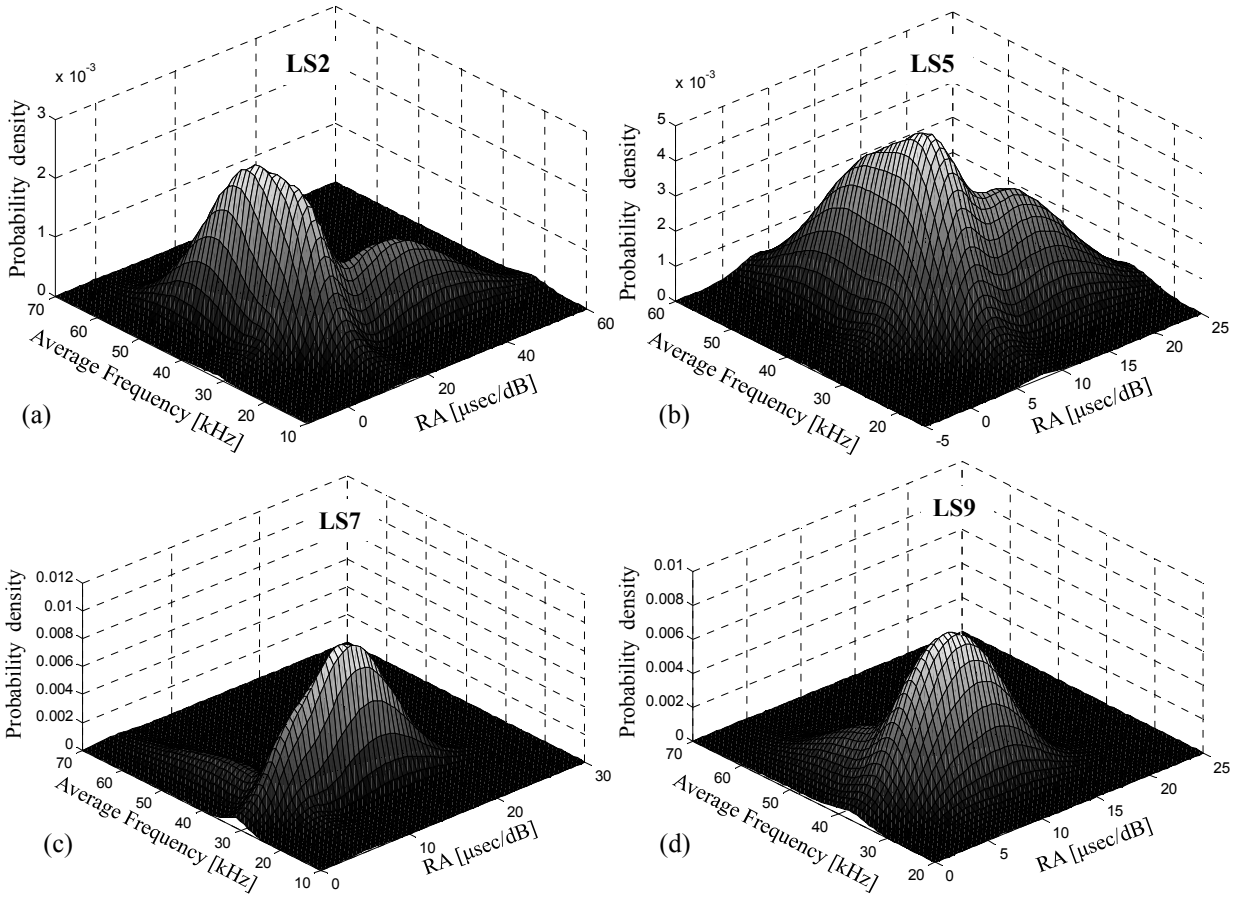

Figure 6. Gaussian Mixture Modeling of clustering parameters for load steps 2, 3 (dominancy of tensile cracks), 5 and 6 (Transition stage from tensile to shear), 7 and 9 (dominancy of shear cracks)

To improve the classification results, a new criterion is proposed to keep the data points with higher probability into the tensile or shear clusters and associate the rest of date set in another cluster namely "Mixed". At this aim, the likelihood ratio test was applied. The discriminate function is based on the log given as,

$$like(\boldsymbol{X}) = p(\lambda_k \mid \boldsymbol{X}) = \frac{N(\boldsymbol{X} \mid \lambda_k)\, p(\lambda_k)}{p(\boldsymbol{X})} = \exp(loglike(\boldsymbol{X})) \tag{10}$$

$$loglike(\boldsymbol{X}) = -\frac{1}{2}(\boldsymbol{X} - \boldsymbol{\mu}_k)^T \sum_k^{-1} (\boldsymbol{X} - \boldsymbol{\mu}_k) + \ln(p(\lambda_k)) - \frac{1}{2}\ln\left|\sum_k\right| - \frac{D}{2}\ln 2\pi \tag{11}$$

$$\psi = -2\ln\frac{like(X)\ for\ 1st Model(Tensile)}{like(X)\ for\ 2nd Model(Shear)} \tag{12}$$

where $\boldsymbol{\psi}$ is the likelihood ratio, $\boldsymbol{\mu_k}$, $\sum_k$, and $p(\lambda_k)$ are the mean, covariance, and weight of the components. The next step is to assign an arbitrary ratio. The value of ψ_T = -1.4 is selected to separate the date in which the likelihood of tensile is twice the likelihood of shear (-2ln(2)=-1.4); likewise, the value of ψ_S=1.4 means the likelihood of shear is twice the likelihood of tensile. Figure 7 illustrates how the likelihood ratio test segregates the dataset in LS5. The diamonds (◊) are tensile signals with higher probability. The gray dots (.) are "Mixed" mode signals since they include the data with less probability of being either shear or tensile. The circles (○) are the shear signals with higher probability. Therefore, the new criterion for boundaries of clusters is defined based on a likelihood ratio value.

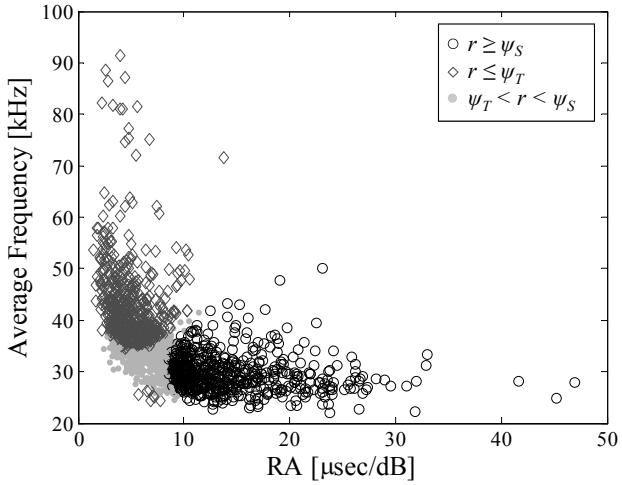

Figure 7. Data selection with higher probability in each cluster for LS5

Figure 8 shows the number of AE signals associated to each cluster versus drift ratio. Below 0.4% drift ratio where the wall was completely elastic (LS5) the majority of AE signals were originated from the nucleation of tensile cracks while after 0.4% drift at LS6, shear signals begin to surpass tensile mode. These observation were confirmed by visual inspection of crack patterns in each load step [5, 7]. Finally, beyond 0.6% drift at load steps 7 to 9, increased number of shear cracks was observed. Another worthy observation can be obtained by comparing these results to the force-displacement hysteresis loops (Figure 3). Onset of yielding occurred in LS7; interestingly the GMM identified high AE activity associated to shear mode in this load step (LS7). The following increase in reported tensile cracks at LS8 can be due to the dominant mechanism of brittle fracture in compression that is basically Mode I cracking, the same as in tension. Under compressive loads, brittle materials fail by the formation of tensile microcracks at microdefects such as cavities and grain interfaces [35]. Table 3 summarizes the ratio of the number of data in each cluster to total data set in each load step. Based on these observations, a Structural Health Monitoring (SHM) system can be designed for similar reinforced concrete shear walls by designating a threshold on the percent of shear mode cracks. The proposed ratio for dominancy of shear class over the other two is 60%. Once the ratio passed that threshold, an early alarm can be triggered as a notice of yielding. Thereafter, imminent failure should be prevented by selecting an appropriate retrofitting scenario.

In addition, this classification scheme allows visualizing how much the classes are intersected. For instance, in LS2, LS7 and LS9 the dominancy of one class of signals is comprehensible while during transition stages (LS5 and LS6) these two classes are highly intersected. Based on these observations we propose a new classification scheme, as shown in Figure 9. The intersection area can be considered as mixed crack mode.

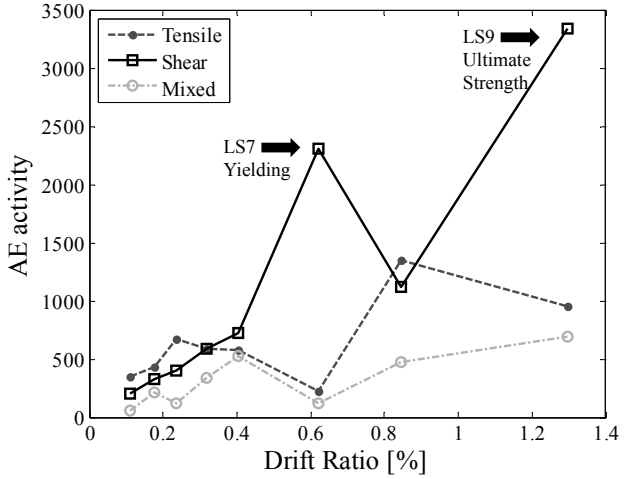

Figure 8. Crack mode activity estimated by GMM

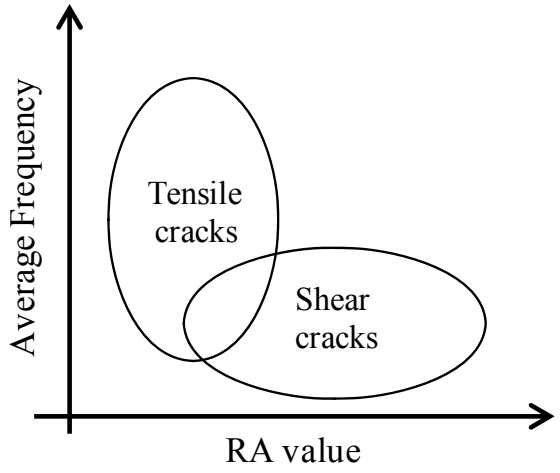

Figure 9. The new classification scheme

Table 3. Percentage of AE activities for each group

Load step	Tensile	Shear	Mixed
2	59%	33%	8%
3	44%	34%	22%
4	56%	34%	10%
5	40%	38%	22%
6	32%	40%	29%
7	20%	**74% warning**	6%
8	46%	38%	16%
9	21%	63%	16%

6. CONCLUSION

This paper presented a new classification approach based on a Gaussian Mixture Modeling (GMM) of acoustic emission for monitoring crack mode (i.e., tensile or shear) in reinforced concrete structures. A full scale RC shear wall was tested to evaluate the robustness and applicability of the proposed system. Acoustic emission waveforms were recorded and two features, RA and Average Frequency (AF), were extracted. These data were used as input to the GMM algorithm to cluster the two hidden classes of shear and tensile. The results shown that three stages in the crack mode progression can be identified: dominancy of tensile cracks at the initial load step, transition stage from tensile to shear, and dominancy of shear cracks at final load steps. Conventional visual inspection confirmed the outcomes of the proposed approach. Further studies should investigate the effects of different aggregate mixture, compressive strength, reinforcement ratio, dimension, AE sensor characteristics, and loading directions (bending, tension, compression) to verify the independency or dependency of the proposed method on each of these factors.

ACKNOWLEDGMENTS

The authors would like to thank Professor Whittaker for allowing us the use of the shear wall experimental setup supported by the National Science Foundation (NSF) under the Grant No. CMMI-0829978. The experiments presented herein could not have been completed without contributions from Mr. B. Luna, and the staff of the Structural Engineering and Earthquake Simulation Laboratory (SEESL) of the State University of New York at Buffalo. The authors also acknowledge the advice and help provided by the technical staff at the NEES Equipment Site at the University at Buffalo.

REFERENCES

[1] Jahanshahi, M. R., Masri, S., Padgett, C., and Sukhatme, G., "An innovative methodology for detection and quantification of cracks through incorporation of depth perception," Mach. Vision Appl. 24, 227-241 (2013).

[2] Gavin, H., Marshall, J., Mayes, R., Gumpertz, S., Springs, C., Tom, C., and Rourke, O., "The M 6.3 Christchurch, New Zealand, Earthquake of February 22 , 2011," EERI Spec. Earthquake Rep. (May), (2011).

[3] DBH, "Christchurch CBD Buildings 22 February 2011 Aftershock Stage 1 Expert Panel Report," New Zealand Department of Building and Housing 3-5 (2011).

[4] Farhidzadeh, A., Salamone, S., Luna, B., and Whittaker, A., "Acoustic Emission Monitoring of a Reinforced Concrete Shear Wall by b-value based Outlier Analysis," Struct. Health Monit.: Int. J. 12(1), 3-13 (2013).

[5] Farhidzadeh, A., Dehghan-Niri, E., Salamone, S., Luna, B., and Whittaker, A., "Monitoring Crack Propagation in Reinforced Concrete Shear Walls by Acoustic Emission," ASCE J. Struct. Eng. (DOI: 10.1061/(ASCE)ST.1943-541X.0000781), (2012).

[6] Rofooei, F., and Farhidzadeh, A., "Investigation on The Seismic Behavior of Steel MRF with Shape Memory Alloy Equipped Connections," Procedia Eng. 14, 3325–3330 (2011).

[7] Farhidzadeh, A., Salamone, S., Dehghan-Niri, E., Luna, B., and Whittaker, A., "Damage Assessment of Reinforced Concrete Shear Walls by Acoustic Emission," NDE/NDT for Highways and Bridges: Structural Materials Technology (SMT) 74–81 (2012).

[8] Farhidzadeh, A., and Salamone, S., "Introducing Sifted b-Value Analysis and a New Crack Classification for Monitoring Reinforced Concrete Shear Walls by Acoustic Emission," 54th Acoustic Emission Working Group Meeting, Princeton, NJ, (Student paper award) 55–57 (2012).

[9] Dehghan Niri, E., Farhidzadeh, A., and Salamone, S., "Adaptive Multisensor Data Fusion for Acoustic Emission (AE) Source Localization in Noisy Environment," Struct Health Monit: Int. J. 12(1), 59–77 (2013).

[10] Dehghan Niri, E., and Salamone, S., "A probabilistic framework for acoustic emission source localization in plate-like structures," Smart Mater. Struct. 21(3), 035009 (2012).

[11] Jahanshahi, M.R., Masri, S.F., and Sukhatme, G.S., "Multi-image stitching and scene reconstruction for evaluating defect evolution in structures," Struct. Health. Monit.: Int. J.10(6), 643–657 (2011).

[12] Jahanshahi, M.R., and Masri, S.F., "A New Methodology for Non-Contact Accurate Crack Width Measurement through Photogrammetry for Automated Structural Safety Evaluation," Smart Mater. Struct. in press, (2013).

[13] Dehghan-Niri, E., Salamone, S., and Singla, P., "Acoustic emission (AE) source localization using extended Kalman filter (EKF)," in Proc. SPIE 8348 (2012).

[14] Salamone, S., Veletzos, M.J., Lanza, F., and Restrepo, J.I., "Detection of Initial Yield and Onset of Failure in Bonded Posttensioned Concrete Beams," ASCE J. Brdg. Eng. 17, 966–974 (2012).

[15] Shiotani, T., Luo, X., Haya, H., and Ohtsu, M., "Damage Quantification for Concrete Structures by Improved b-Value Analysis of AE," Earthquakes and Acoustic Emission 1, 181–186 (2007).

[16] Benavent-Climent, A., Gallego, A., and Vico, J.M., "An acoustic emission energy index for damage evaluation of reinforced concrete slabs under seismic loads," Struct. Health. Monit.: Int J. 11(1), 69–81 (2011).

[17] Bilmes, J.A., "A Gentle Tutorial of the EM Algorithm and its Application to Parameter Estimation for Gaussian Mixture and Hidden Markov Models", Int. Comp. Sci. Inst., Berkeley, California (1998).

[18] Reynolds, D.A., and Rose, R.C., "Robust Text-Inependent Speaker Identification Using Gaussian Mixture Speaker Models," IEEE T. Speech. Audi. P. 3(1), 72–83 (1995).

[19] Reynolds, D. a., Quatieri, T.F., and Dunn, R.B., "Speaker Verification Using Adapted Gaussian Mixture Models," Digit. Signal Process. 10(1-3), 19–41 (2000).

[20] Permuter, H., Francos, J., and Jermyn, I., "A study of Gaussian mixture models of color and texture features for image classification and segmentation," Pattern Recogn. 39(4), 695–706 (2006).

[21] Terejanu, G., Singla, P., Singh, T., and Scott, P.D., "Uncertainty Propagation for Nonlinear Dynamic Systems Using Gaussian Mixture Models," J. Guid. Control Dynam. 31(6), 1623–1633 (2008).

[22] Richiardi, J., and Drygajlo, A., "Gaussian Mixture Models for on-line signature verification," Proc. ACM SIGMM workshop on Biometrics methods and applications - WBMA 115-122 (2003).

[23] Norouzi, M., Kumpf, J., Hunt, V., and Helmicki, A., "An Integrated Monitor and Warning System for the Jeremiah Morrow Bridge," in NDE/NDT for Highways and Bridges Structural Materials Technology (SMT), 250–258 (2012).

[24] JCMS-IIIB5706, "Japan Construction Material Standards. Monitoring Method for Active Cracks in Concrete by Acoustic Emission," Japan: The Federation of Construction Material Industries (2003).

[25] Soulioti, D., Barkoula, N.M., Paipetis, a., Matikas, T.E., Shiotani, T., and Aggelis, D.G., "Acoustic emission behavior of steel fibre reinforced concrete under bending," Constr. Build. Mater. 23(12), 3532–3536 (2009).
[26] Ohtsu, M., and Tomoda, Y., "Phenomenological Model of Corrosion Process in Reinforced Concrete Identified by Acoustic Emission," ACI Mater J 105(2), 194–199 (2008).
[27] Ohno, K., and Ohtsu, M., "Crack classification in concrete based on acoustic emission," Constr. Build. Mater. 24(12), 2339–2346 (2010).
[28] Ohtsu, M., "Recommendation of RILEM TC 212-ACD: acoustic emission and related NDE techniques for crack detection and damage evaluation in concrete," RILEM Tech. Committee 43(9), 1187–1189 (2010).
[29] Aggelis, D.G., "Classification of cracking mode in concrete by acoustic emission parameters," Mech. Res. Commun. 38(3), 153–157 (2011).
[30] Hastie, T., Tibshirani, R., and Friedman, J., "The Elements of Statistical Learning" , 2nd ed., Springer. pp., 272–279 (2008).
[31] Dempster, A.P., Laird, N.M., and Rubin, D.B., "Maximum Likelihood from Incomplete Data via the EM Algorithm," J. R. Stat. Soc. 39(1), 1–38 (1977).
[32] Rabiner, L.R., and Juang, B.H., "An Introduction to Hidden Markov Models," IEEE ASSP Mag. (Jan.), pp. 4–16 (1986).
[33] Rammohan, R., and Taha, M.R., "Exploratory Investigations for Intelligent Damage Prognosis using Hidden Markov Models," 2005 IEEE Trans. Syst., Man, Cybern., Syst. 2, 1524–1529 (2005).
[34] ACI Committee 318, "Building Code Requirements for Structural Concrete and Commentary (ACI 318-08)," (2008).
[35] Nemat-Nasser, S., and Hori, M., "Micromechanics: Overall properties of heterogeneous materials," North-Holland, Amsterdam. (1993).